Backbone NMR resonance assignment of the apo human Tsg101-UEV domain

Danai Moschidi, François-Xavier Cantrelle, Emmanuelle Boll, Xavier Hanoulle

Backbone NMR resonance assignment of the apo human Tsg101-UEV domain

Danai Moschidi, François-Xavier Cantrelle, Emmanuelle Boll & Xavier Hanoulle*

[1] CNRS EMR9002 Integrative Structural Biology, F-59000, Lille, France
[2] Univ. Lille, Inserm, CHU Lille, Institut Pasteur de Lille, U1167 - RID-AGE - Risk Factors and Molecular Determinants of Aging-Related Diseases, F-59000, Lille, France

**Corresponding author:*
Xavier Hanoulle
xavier.hanoulle@univ-lille.fr
ORCID: 0000-0002-3755-2680

Abstract

The Endosomal Sorting Complex Required for Transport (ESCRT) pathway, through inverse topology membrane remodeling, is involved in many biological functions, such as ubiquitinated membrane receptor trafficking and degradation, multivesicular bodies (MVB) formation and cytokinesis. Dysfunctions in ESCRT pathway have been associated to several human pathologies, such as cancers and neurodegenerative diseases. The ESCRT machinery is also hijacked by many enveloped viruses to bud away from the plasma membrane of infected cells. Human tumor susceptibility gene 101 (Tsg101) protein is an important ESCRT-I complex component. The structure of the N-terminal ubiquitin E2 variant (UEV) domain of Tsg101 (Tsg101-UEV) comprises an ubiquitin binding pocket next to a late domain [P(S/T)AP] binding groove. These two binding sites have been shown to be involved both in the physiological roles of ESCRT-I and in the release of the viral particles, and thus are attractive targets for antivirals. The structure of the Tsg101-UEV domain has been characterized, using X-ray crystallography or NMR spectroscopy, either in its apo-state or bound to ubiquitin or late domains. In this study, we report the backbone NMR resonance assignments, including the proline signals, of the apo human Tsg101-UEV domain, that so far was not publicly available. These data, that are in good agreement with the crystallographic structure of Tsg101-UEV domain, can therefore be used for further NMR studies, including protein-protein interaction studies and drug discovery.

Keywords: Tsg101 protein · UEV domain · Backbone Assignments · Proline Assignments · NMR Spectroscopy · Molecular interactions

Biological context

Human tumor susceptibility gene 101 protein (Tsg101 protein) is one of the components of the Endosomal Sorting Complex Required for Transport (ESCRT) machinery that is highly conserved in eukaryotes. The ESCRT pathway is involved in the sorting, trafficking and lysosomal degradation of ubiquitinated proteins through the multivesicular bodies (MVB), but it is also involved in many others biological processes, such as membrane recycling, cytokinesis, autophagy or exosome secretion (Williams and Urbé 2007; Henne et al. 2011). In these physiological processes, ESCRTs mediate inverse membrane remodeling with the formation of vesicles which contain cytosol and bud away from it, either at cell surface or inside cellular organelles (Flower et al. 2020).

The ESCRT machinery comprises five different multi-subunit complexes (ESCRT-0, -I, -II, -III and the Vps4 complex) that assemble on the cytosolic side of the membrane (Schmidt and Teis 2012; Vietri et al. 2020). ESCRT-0 initiates the recognition of the ubiquitinated proteins and establishes interactions with both lipids (phosphatidylinositol3-phosphate, PI3P) and proteins. The hepatocyte growth factor (HGF)-regulated Tyrosine kinase substrate (HRS) from ESCRT-0 establishes a direct protein-protein interaction with Tsg101 that belongs to ESCRT-I. The assembly of Tsg101 with Vps28, Vps37 (A, B, C, D) and Mvb12 (A, B) or ubiquitin-associated protein 1 (UBAP1) constitutes the hetero-tetrameric ESCRT-I. The latter one recruits ESCRT-II that is a hetero-tetrameric complex with a GLUE domain that can simultaneously bind to Vps28 from ESCRT-I, ubiquitin and PI3P. Then, ESCRT-II recruits ESCRT-III, a multimeric complex made of charged multivesicular body proteins (CHMP) and accessory proteins. This complex, in contrast to the other ones, will transiently assemble and constitute the main driving force with the AAA-ATPase Vps4 for membrane constriction and scission (Vietri et al. 2020).

The ESCRT machinery, by controlling the membrane proteins recycling, allows the tight regulation of cell receptors signaling. As a consequence of this central regulation mechanism, altered ESCRT functions have been associated with many human diseases, such as cancers and neurodegenerative diseases (Ferraiuolo et al. 2020). Moreover, it has been shown that the ESCRT machinery is a host factor that is required for the replication cycle of some viruses. Indeed, many enveloped RNA viruses, such as HIV-1 (VerPlank et al. 2001; Garrus et al. 2001), Ebola (Martin-Serrano et al. 2001), human T-lymphotropic virus (Bouamr et al. 2003) or HEV (Nagashima et al. 2011), hijack the ESCRT pathway to bud away from the plasma membrane of infected cells, a process that is similar to vesicles budding into intracellular organelles from the cytosol. Whereas ESCRT-0 and -II seem dispensable, ESCRT-I and -III have been shown to be involved in viral particles maturation and release. A key player in this process is the Tsg101 protein from ESCRT-I.

The Tsg101 protein (Vps23 in yeast) is a ~44 kDa protein that is composed of several domains. From the N-terminus to the C-terminus, there are a ubiquitin E2 variant (UEV) domain, a proline-rich region (PRR), a Stalk domain and a Head domain (Flower et al. 2020). Both the Stalk and Head domains of Tsg101 are components of the ESCRT-I core that displays an elongated rod-like shape structure (Boura et al. 2011). The N-terminal UEV domain of Tsg101 (residues 2-145) protrudes from the ESCRT-I core to which it is connected via a disordered and flexible

PRR. The Tsg101 UEV domain (Tsg101-UEV) binds ubiquitin, but is devoid of enzymatic E2 ligase activity as the catalytic cysteine residue is absent (Pornillos et al. 2002b). This interaction allows ESCRT-I to bind ubiquitinated cargo that have to be processed through the MVB pathway. Next to this ubiquitin-binding pocket, there is a groove at the surface of Tsg101-UEV that interacts with P(S/T)AP peptide sequence. This is how ESCRT-I interacts with ESCRT-0, in which HRS displays a PSAP peptide sequence. Tsg101 biological functions are auto-regulated by an interaction between an internal PTAP motif and its Tsg101-UEV domain (Lu et al. 2003; McDonald and Martin-Serrano 2008). Several viruses, such as HIV-1, Ebola, HEV and Marburg virus (MARV), have been shown to recruit ESCRT-I at their assembly/budding sites through interaction of Tsg101-UEV with viral late domains [P(T/S)AP] (Freed 2002; Pornillos et al. 2002a; Dolnik et al. 2014). These latter ones are located in the HIV-1 Gag, Ebola VP40, HEV ORF3 and MARV NP proteins. This protein-protein interaction thus constitutes an attractive drug target to develop antivirals. Peptidomimetics, including cyclic peptides (Tavassoli et al. 2008; Lennard et al. 2019) and small molecules (Siarot et al. 2018), have indeed been shown to abolish the interaction between HIV-1 Gag and human Tsg101-UEV and to interfere with viral particles release. In addition, prazole-based drugs abolishing the ubiquitin binding function of Tsg101-UEV proved to interfere with the early HIV-1 assembly, independently of its interaction with the HIV-1 Gag PTAP late domain (Strickland et al. 2017). More recently, tenatoprazole and ilaprazole have been shown to inhibit the release of HIV-1 and Herpes Simplex Virus (HSV) 1/2 infectious particles from infected cells (Leis et al. 2021). Two contiguous binding pockets in Tsg101-UEV could thus be targeted to develop broad-spectrum antivirals against enveloped viruses.
Here, we report the backbone ($^{13}C_\alpha$, $^{13}C_\beta$, ^{13}CO, $^{15}N^H$, $^1H^N$, $^1H_\alpha$) assignments, including the proline ($^{13}C_\alpha$, $^{13}C_\beta$, ^{13}CO, ^{15}N ,$^1H_\alpha$) assignments, of human Tsg101-UEV domain in its apo-state. These data could be further used to study the molecular details of Tsg101-UEV interactions with protein partners, as well as its structural/conformational consequences, or for drug screening purpose. In this case, the assignments give the possibility to distinguish the P(S/T)AP and ubiquitin binding pockets.

Methods and experiments

Protein expression and purification

The DNA sequence coding for the human UEV domain of Tsg101 (residues 1-145) (Uniprot accession number Q99816) was synthesized, with codon optimization for *E. coli*, by GeneCust and inserted into pET28a(+) plasmid between the *Nco*I and *Bam*HI restriction sites to give the pET28a-Tsg101-UEV plasmid. The coding sequence has been designed to produce the Tsg101-UEV domain with an His_6-tag at its N-terminus followed by a Tobacco Etch Virus (TEV) cleavage site. Thus, the amino-acid sequence of the recombinant protein corresponds to GSSHHHHHHSSG*ENLYFQ/GA*-(Tsg101-UEV residue 1-145). The pET28a-Tsg101-UEV plasmid was transformed into *E. coli* BL21(DE3) cells for overexpression.

Few colonies from a *Luria-Bertani* (LB)-agar plate supplemented with kanamycin (25 µg/mL) were used to inoculate 25 mL of LB medium. Bacteria were grown overnight at 37°C with shaking. Then, 20 mL of this pre-culture were added in 1 L of an optimized M9 minimal medium containing 1 g/L $^{15}NH_4Cl$, 3 g/L $^{13}C_6$-D-glucose and 0.5 g/L ISOGRO-^{15}N,^{13}C (Sigma-Aldrich) supplemented with kanamycin (25 µg/mL). The cells were grown at 37°C, at 160 rpm, until the OD_{600} reached ~1.0 and then the protein expression was induced by addition of 0.4 mM isopropyl-β-D-thiogalactopyranoside (IPTG). After 4-5 hours at 37°C, the cells were harvested by centrifugation at 5,000 x *g* for 20 min at 4°C. The cell pellet was resuspended in 40 mL of Buffer R (50 mM Na_2HPO_4/NaH_2PO_4 (NaPi) pH 7.8, 500 mM NaCl, 10 mM Imidazole) supplemented with EDTA-free protease inhibitor cocktail (cOmplete, Roche, 1 tablet), DNaseI (150 µL at 6 mg/mL) and RNaseA (15 µL at 40 mg/mL). The cell lysis was done using an homogenizer (EmulsiFlexC3, Avestin), with 5 passages at 20,000 psi at 4°C. The cell extract was centrifuged at 39,000 x *g* for 40 min at 4°C. After filtration (0.45 µm), the supernatant was loaded on a HisTrapHP column (1 mL, Cytiva) to purify the isotopically labeled UEV domain of Tsg101 protein, thanks to the N-terminal His_6-tag. The protein bound to the affinity column was eluted using a linear gradient with increasing concentration of Imidazole (from 10 to 300 mM Imidazole in 15 column volume) while 0.8 mL elution fractions were collected. The elution fractions were analyzed by SDS-PAGE (4-20%) and Coomassie staining. The fractions containing Tsg101-UEV were pooled, supplemented with TEV protease (500 µL at 5 mg/mL) and dialyzed (6-8 kDa cut-off) overnight at 15°C against Buffer D (50 mM Tris-HCl pH 6.4, 250 mM NaCl, 5 mM β-mercaptoethanol). This allowed for simultaneous His_6-tag cleavage and Imidazole removal. Then, the cleaved protein was loaded on the HisTrapHP column to remove both the cleaved His_6-tag and the TEV protease. The Tsg101-UEV domain was then dialyzed (6-8 kDa cut-off) overnight at 4°C against NMR Buffer (50 mM NaPi pH 6.1, 50 mM NaCl, 0.1 mM

EDTA) and finally concentrated to 330 µM. The doubly labeled $^{15}N,^{13}C$-Tsg101-UEV protein was flash frozen in liquid Nitrogen and stored at -80^{o}C until used.

NMR sample and NMR data acquisition and processing

A doubly labeled $^{15}N,^{13}C$ Tsg101-UEV sample at 330 µM concentration was placed into a 5 mm Shigemi tube (300 µL) to record all the NMR experiments, at 298 K, using a 600 MHz Bruker spectrometer (Avance III HD) equipped with a CPQCI cryoprobe. The sample was in NMR Buffer (50 mM NaPi pH 6.1, 50 mM NaCl, 0.1 mM EDTA) and was supplemented with 5% (*v*/*v*) D_2O and Trimethyl Silyl Propionate (TMSP).

The classical backbone assignments were obtained from 3D experiments CBCANH, HNCO, CBCACONH, HN(CA)CO, HNHA and HN(CA)NNH, while the assignments of prolines resonances were based on the carbon-detected 3D hCACON and HCAN and the 2D NCO and CACO experiments. All 3D spectra were recorded using non-uniform sampling (Table 1). The data were acquired and processed using Topspin 3.5 (Bruker Biospin). The TMSP signal was used as the ^{1}H chemical shift reference, and the ^{15}N and ^{13}C chemical shifts were indirectly referenced based on ^{1}H chemical shifts. The NMR data were analyzed using NMRFAM-Sparky (Lee et al. 2015) and checked by I-PINE web server (Lee et al. 2019).

Table 1 List of NMR experiments acquired at 600 MHz spectrometer and corresponding parameters that have been used for Tsg101-UEV assignment.

	Time domain data size (points)			Spectral width/Carrier frequency (ppm)			NS	Delay time (s)	NUS points	NUS (%)
	t1	t2	t3	F1	F2	F3				
$^{1}H,^{15}N$ HSQC	2048	256		14/4.7 (^{1}H)	28/117.5 (^{15}N)		16	1	64	50
CBCANH	2048	82	120	14/4.7 (^{1}H)	28/117.5 (^{15}N)	60/42 (^{13}C)	48	1	688	28
CBCACONH	2048	82	120	14/4.7 (^{1}H)	28/117.5 (^{15}N)	60/42 (^{13}C)	48	1	590	24
HNCO	1432	82	128	12/4.7 (^{1}H)	30/118 (^{15}N)	11/173 (^{13}C)	16	0.25	419	16
HNCACO	1426	82	128	12/4.7 (^{1}H)	28/ 117.5 (^{15}N)	14/173.5 (^{13}C)	64	0.25	524	20
HN(CA)NNH	2048	128	128	14/4.7 (^{1}H)	28/117.5 (^{15}N)	28/117.5 (^{15}N)	48	1	491	12
HACAN	2048	128	128	14/4.7 (^{1}H)	40/52 (^{13}C)	28/117.5 (^{15}N)	32	1	737	18
HNHA	2048	256	128	14/4.7 (^{1}H)	12/4.7 (^{1}H)	28/117.5 (^{15}N)	32	1	491	6
hCACON	1024	128	64	40/173.5 (^{13}C)	43/123 (^{15}N)	40/173.5 (^{13}C)	32	1	409	20
$^{13}C,^{15}N$ NCO	1024	160		40/173.5 (^{13}C)	47/123 (^{15}N)		160	1	40	50
$^{13}C,^{13}C$ CACO	724	256		20/173.5 (^{13}C)	50/173.5 (^{13}C)		160	1	32	50

Extent of assignments and data deposition

After TEV cleavage, two extra residues from the purification tag were present at the N-terminus of the protein. These were not taken into account for both the assignment and the sequence numbering purpose. Therefore, the first residue (residue 1) is the methionine (Met) of human Tsg101-UEV domain. The advantage of the presence of these extra residues was that even the resonances corresponding to the first N-terminal residues of the Tsg101-UEV were observed in the $^{1}H,^{15}N$ HSQC spectrum.

The 2D $^{1}H,^{15}N$ HSQC spectrum of the apo form of Tsg101-UEV domain (residues 1-145 of the full-length protein) displays well dispersed resonances with almost no overlap. All backbone ^{1}H-^{15}N resonances in the $^{1}H,^{15}N$ HSQC spectrum were successfully assigned except the one corresponding to residue Asn45 (N45) that was not visible (Fig. 1, 99% completeness). We also successfully assigned all backbone ^{15}N-^{13}CO resonances in the 2D $^{15}N,^{13}C$-NCO spectrum in which a correlation can be observed for each protein residue, including the 13 proline residues with their corresponding resonances located in the ^{15}N 131-143 ppm region of the spectrum (Fig. 2, completeness 100%).

Overall, the analysis of our full NMR dataset resulted in the assignment of 131 out of 132 backbone ^{1}H-^{15}N correlations (99%), 138 out of 145 $^{1}H_{\alpha}$ resonances (95%), 145 out of 145 backbone $^{15}N^{H}$ and $^{13}C_{\alpha}$ resonances (100%), 133 out of 138 $^{13}C_{\beta}$ resonances (96%), 144 out of 145 ^{13}CO resonances (99%) and 145 out of 145 $^{1}H_{\alpha}$ resonances (100%) [2 of the 7 glycine residues have only one $^{1}H_{\alpha}$ resonance]. In addition, the ^{1}H-^{15}N correlations, in the ^{1}H,^{15}N HSQC spectrum, arising from side chains of Asn, Gln and Trp residues were also assigned (Fig. 1) Only for Asn54 we could not determine the $^{13}C_{\gamma}$, $^{15}N_{\delta 2}$ and $^{1}H_{\delta 2}$ resonances. Regarding the 13 prolines residues, all the ^{15}N, $^{13}C_{\alpha}$, $^{1}H_{\alpha}$, $^{13}C_{\beta}$ and ^{13}CO (except the one from Pro145) signals were assigned and we also assigned 7 out of 13 $^{13}C_{\delta}$ and $^{1}H_{\delta 2/3}$ resonances (54%) using the 3D HCAN spectrum. The analysis of the $^{13}C_{\beta}$ chemical shift of prolines showed that two proline residues, Pro81 and Pro120, are in *cis* conformation with their $^{13}C_{\beta}$ value being close to ~34 ppm. This observation is in agreement with the crystal structure of the Tsg101-UEV domain (PDB entry 2F0R) in which these two prolines are referred as *cis*-peptides (Palencia et al. 2006). Two proline residues, Pro81 and Pro84, display unusual chemical shifts. Based on the crystallographic structure, we attributed this to the close packing with surrounding aromatic residues (Trp117, Tyr80, Tyr82 and His119). Moreover, Pro84 is part of a Pro-Pro motif in the sequence. All the assigned chemical shifts have been deposited in the Biological Magnetic Resonance Bank (https://bmrb.io/) under the accession number 50765.

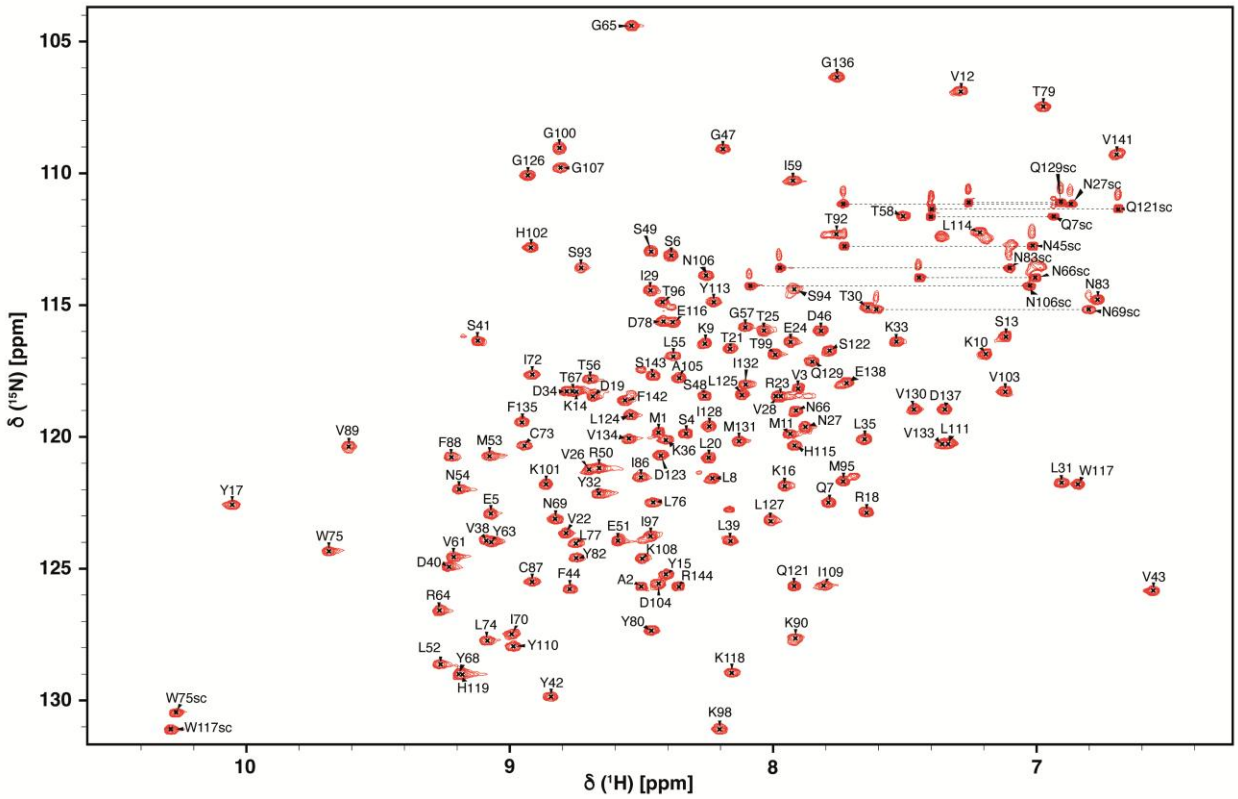

Fig. 1 Annotated 2D ^{1}H,^{15}N HSQC spectrum of apo human Tsg101-UEV domain. The resonance assignments are shown with black labels. Resonances corresponding to Asn, Gln and Trp side-chains are annotated with a "sc" label

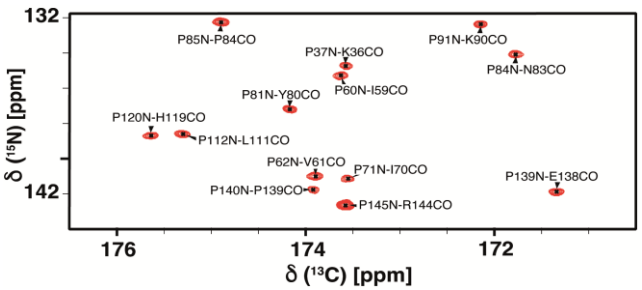

Fig. 2 Annotated 2D carbon-detected ^{15}N,^{13}C-NCO spectrum of apo human Tsg101-UEV domain. The spectrum is centered on the proline region (132-143 ppm for the ^{15}N dimension). The resonance assignments are shown with black labels

Using the backbone NMR chemical shifts, we analyzed the secondary structure content in the apo Tsg101-UEV domain using both the CSI 3.0 (Hafsa et al. 2015) web server and the Secondary Structure Propensities (SSP) program (Marsh et al. 2006). Both the CSI and SSP methods gave similar results. The results were compared with the secondary structures from the crystal structure of the Tsg101-UEV domain (PDB entry 2F0R) (Palencia et al. 2006) and proved to be well correlated (Fig. 3). A short α-helix (residues 111-116) was not identified using CSI 3.0 because of its lower propensity highlighted by the ~0.4 SSP score (Fig. 3b,c). Moreover, the flexibility of the apo Tsg101-UEV domain in solution was predicted from the experimental NMR chemical shifts using TALOS+ server (Shen et al. 2009). The Random Coil Index (RCI) derived S^2 values for all residues are shown in Fig.3c (blue dots) and matched with the increase flexibility observed for the N- and C-termini and the loops connecting the secondary structures of Tsg101-UEV domain.

The assignments of the apo Tsg101-UEV domain may be used for drug screening purposes or to perform in-depth study of any molecular interaction with others molecular partners, such as peptides or proteins.

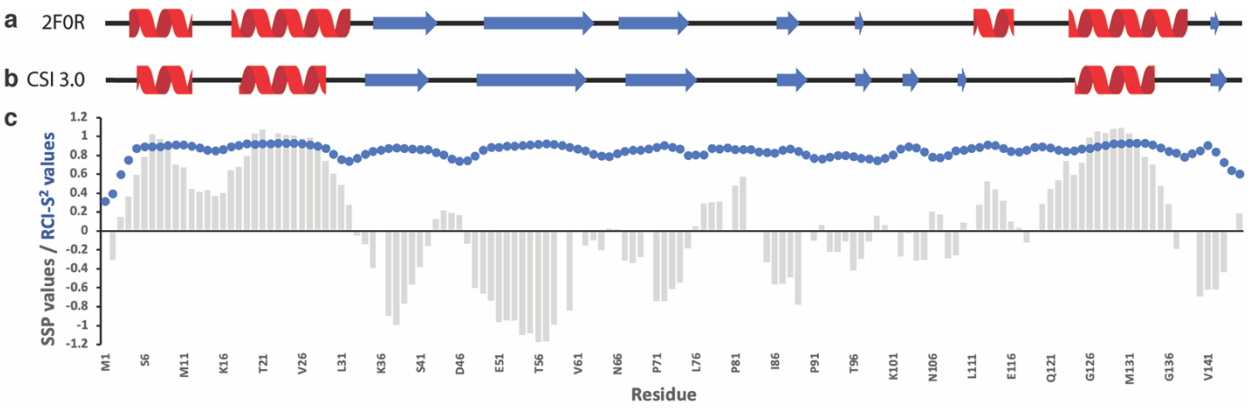

Fig. 3 Secondary structure analysis and flexibility of Tsg101-UEV domain. (a) Secondary structure analysis from the crystal structure of Tsg101-UEV domain (PDB ID 2F0R) (Palencia et al. 2006; Hafsa et al. 2015). (b) Secondary structure analysis based on the experimental backbone NMR chemical shifts ($^1H^N$, $^{15}N^H$, $^{13}C_\alpha$, $^1H_\alpha$, $^{13}C_\beta$ and ^{13}CO) of the protein using the CSI 3.0 web server (Hafsa et al. 2015). Red cartoon represents the α-helix and blue arrow the β-strand. (c) Secondary Structure Propensities (SSP) score values (grey bars) based on $^{13}C_\alpha$, $^{13}C_\beta$ and $^1H_\alpha$ chemical shifts of human Tsg101-UEV domain (Marsh et al. 2006). Positive and negative values indicate α-helix and extended structure propensities, respectively. The flexibility of the protein is highlighted by the predicted order parameter (Random Coil Index S^2, RCI-S^2, blue dots) based on the backbone chemical shifts ($^1H^N$, $^{15}N^H$, $^{13}C_\alpha$, $^1H_\alpha$, $^{13}C_\beta$ and ^{13}CO) using the TALOS+ server (Shen et al. 2009)

Declarations

Ethics approval and consent to participate
Not applicable

Consent for publication
All authors have agreed to the publication of the manuscript.

Availability of data and material
All the chemical shift values of apo human Tsg101-UEV domain were deposited in the Biological Magnetic Resonance Data Bank (BMRB) under accession code 50765.

Competing interests
The authors declare that they have no conflict of interest.

Funding
This study was supported by the French National Agency for Research on AIDS and Viral Hepatitis (ANRS) Grant ECTZ101316, and a PhD fellowship from ANRS to D.M. (ECTZ103422).

Authors' contributions
D.M. and X.H performed protein expression and purification. F-X.C. and E.B. collected the NMR data. D.M. analysed the data and wrote the first draft of the manuscript. D.M. prepared figures 1-3. All authors commented on previous versions of the manuscript. All authors reviewed the manuscript. Funding acquisition and supervision were done by X.H.

Authors' information (optional)
Not applicable

Acknowledgements
The NMR facilities were funded by the Nord Region Council, CNRS, Institut Pasteur de Lille, European Union (FEDER), French Research Ministry and University of Lille. Financial support from the NMR division of Infranalytics (FR 2054 CNRS) is gratefully acknowledged.

References

Bouamr F, Melillo JA, Wang MQ, et al (2003) PPPYEPTAP Motif Is the Late Domain of Human T-Cell Leukemia Virus Type 1 Gag and Mediates Its Functional Interaction with Cellular Proteins Nedd4 and Tsg101. J Virol 77:11882–11895. https://doi.org/10.1128/JVI.77.22.11882-11895.2003

Boura E, Różycki B, Herrick DZ, et al (2011) Solution structure of the ESCRT-I complex by small-angle X-ray scattering, EPR, and FRET spectroscopy. Proc Natl Acad Sci 108:9437–9442. https://doi.org/10.1073/pnas.1101763108

Dolnik O, Kolesnikova L, Welsch S, et al (2014) Interaction with Tsg101 Is Necessary for the Efficient Transport and Release of Nucleocapsids in Marburg Virus-Infected Cells. PLoS Pathog 10:e1004463. https://doi.org/10.1371/journal.ppat.1004463

Ferraiuolo R-M, Manthey KC, Stanton MJ, et al (2020) The Multifaceted Roles of the Tumor Susceptibility Gene 101 (TSG101) in Normal Development and Disease. Cancers 12:450. https://doi.org/10.3390/cancers12020450

Flower TG, Takahashi Y, Hudait A, et al (2020) A helical assembly of human ESCRT-I scaffolds reverse-topology membrane scission. Nat Struct Mol Biol 27:570–580. https://doi.org/10.1038/s41594-020-0426-4

Freed EO (2002) Viral Late Domains. J Virol 76:4679–4687. https://doi.org/10.1128/JVI.76.10.4679-4687.2002

Garrus JE, von Schwedler UK, Pornillos OW, et al (2001) Tsg101 and the Vacuolar Protein Sorting Pathway Are Essential for HIV-1 Budding. Cell 107:55–65. https://doi.org/10.1016/S0092-8674(01)00506-2

Hafsa NE, Arndt D, Wishart DS (2015) CSI 3.0: a web server for identifying secondary and super-secondary structure in proteins using NMR chemical shifts. Nucleic Acids Res 43:W370–W377. https://doi.org/10.1093/nar/gkv494

Henne WM, Buchkovich NJ, Emr SD (2011) The ESCRT Pathway. Dev Cell 21:77–91. https://doi.org/10.1016/j.devcel.2011.05.015

Lee W, Bahrami A, Dashti HT, et al (2019) I-PINE web server: an integrative probabilistic NMR assignment system for proteins. J Biomol NMR 73:213–222. https://doi.org/10.1007/s10858-019-00255-3

Lee W, Tonelli M, Markley JL (2015) NMRFAM-SPARKY: enhanced software for biomolecular NMR spectroscopy. Bioinforma Oxf Engl 31:1325–1327. https://doi.org/10.1093/bioinformatics/btu830

Leis J, Luan C-H, Audia JE, et al (2021) Ilaprazole and Other Novel Prazole-Based Compounds That Bind Tsg101 Inhibit Viral Budding of Herpes Simplex Virus 1 and 2 and Human Immunodeficiency Virus from Cells. J Virol 95:e00190-21. https://doi.org/10.1128/JVI.00190-21

Lennard KR, Gardner RM, Doigneaux C, et al (2019) Development of a Cyclic Peptide Inhibitor of the p6/UEV Protein–Protein Interaction. ACS Chem Biol 14:1874–1878. https://doi.org/10.1021/acschembio.9b00627

Lu Q, Hope LW, Brasch M, et al (2003) TSG101 interaction with HRS mediates endosomal trafficking and receptor down-regulation. Proc Natl Acad Sci 100:7626–7631. https://doi.org/10.1073/pnas.0932599100

Marsh JA, Singh VK, Jia Z, Forman-Kay JD (2006) Sensitivity of secondary structure propensities to sequence differences between α- and γ-synuclein: Implications for fibrillation. Protein Sci 15:2795–2804. https://doi.org/10.1110/ps.062465306

Martin-Serrano J, Zang T, Bieniasz PD (2001) HIV-1 and Ebola virus encode small peptide motifs that recruit Tsg101 to sites of particle assembly to facilitate egress. Nat Med 7:1313–1319. https://doi.org/10.1038/nm1201-1313

McDonald B, Martin-Serrano J (2008) Regulation of Tsg101 Expression by the Steadiness Box: A Role of Tsg101-associated Ligase. Mol Biol Cell 19:754–763. https://doi.org/10.1091/mbc.e07-09-0957

Nagashima S, Takahashi M, Jirintai S, et al (2011) Tumour susceptibility gene 101 and the vacuolar protein sorting pathway are required for the release of hepatitis E virions. J Gen Virol 92:2838–2848. https://doi.org/10.1099/vir.0.035378-0

Palencia A, Martinez JC, Mateo PL, et al (2006) Structure of human TSG101 UEV domain. Acta Crystallogr D Biol Crystallogr 62:458–464. https://doi.org/10.1107/S0907444906005221

Pornillos O, Alam SL, Davis DR, Sundquist WI (2002a) Structure of the Tsg101 UEV domain in complex with the PTAP motif of the HIV-1 p6 protein. Nat Struct Mol Biol 9:812–817. https://doi.org/10.1038/nsb856

Pornillos O, Alam SL, Rich RL, et al (2002b) Structure and functional interactions of the Tsg101 UEV domain. EMBO J 21:2397–2406. https://doi.org/10.1093/emboj/21.10.2397

Schmidt O, Teis D (2012) The ESCRT machinery. Curr Biol 22:R116–R120. https://doi.org/10.1016/j.cub.2012.01.028

Shen Y, Delaglio F, Cornilescu G, Bax A (2009) TALOS+: a hybrid method for predicting protein backbone torsion angles from NMR chemical shifts. J Biomol NMR 44:213–223. https://doi.org/10.1007/s10858-009-9333-z

Siarot L, Chutiwitoonchai N, Sato H, et al (2018) Identification of human immunodeficiency virus type-1 Gag-TSG101 interaction inhibitors by high-throughput screening. Biochem Biophys Res Commun 503:2970–2976. https://doi.org/10.1016/j.bbrc.2018.08.079

Strickland M, Ehrlich LS, Watanabe S, et al (2017) Tsg101 chaperone function revealed by HIV-1 assembly inhibitors. Nat Commun 8:1391. https://doi.org/10.1038/s41467-017-01426-2

Tavassoli A, Lu Q, Gam J, et al (2008) Inhibition of HIV Budding by a Genetically Selected Cyclic Peptide Targeting the Gag−TSG101 Interaction. ACS Chem Biol 3:757–764. https://doi.org/10.1021/cb800193n

VerPlank L, Bouamr F, LaGrassa TJ, et al (2001) Tsg101, a homologue of ubiquitin-conjugating (E2) enzymes, binds the L domain in HIV type 1 Pr55Gag. Proc Natl Acad Sci 98:7724–7729. https://doi.org/10.1073/pnas.131059198

Vietri M, Radulovic M, Stenmark H (2020) The many functions of ESCRTs. Nat Rev Mol Cell Biol 21:25–42. https://doi.org/10.1038/s41580-019-0177-4

Williams RL, Urbé S (2007) The emerging shape of the ESCRT machinery. Nat Rev Mol Cell Biol 8:355–368. https://doi.org/10.1038/nrm2162